# Characterization of the Human Cytomegalovirus Protease As an Induced-Fit Serine Protease and the Implications to the Design of Mechanism-Based Inhibitors

**Steven R. LaPlante, Pierre R. Bonneau, Norman Aubry, Dale R. Cameron, Robert Déziel, Chantal Grand-Maître, Céline Plouffe, Liang Tong,[†] and Stephen H. Kawai***

*Contribution from the Departments of Chemistry and Biological Sciences, Boehringer Ingelheim (Canada) Ltd., Bio-Méga Research Division, Laval, Quebec H7S 2G5, Canada*

*Received November 10, 1998*

**Abstract:** The conformational properties of the *N-tert*-butylacetyl-L-*tert*-butylglycyl-L-$N^\delta$,$N^\delta$-dimethylasparagyl-L-alanyl methyl ketone (MK) **1** and its terminal *N*-isopropylacetyl analogue **2** were investigated. Whereas these compounds are weak (mM $IC_{50}$ range) inhibitors of the human cytomegalovirus (HCMV) protease, their activated carbonyl analogues are >1000-fold more potent (e.g., trifluoromethyl ketone **3**, $IC_{50}$ = 1.1 $\mu$M). A combination of NMR techniques demonstrated that MK **2** exists in solution as a relatively rigid and extended peptide structure and that the bulky side chains, notably the P3 *tert*-butyl group, greatly contribute to maintaining this solution conformation. Furthermore, transferred nuclear Overhauser effect (TRNOE) studies provided an enzyme-bound conformation of MK **2** that was found to be similar to its free solution structure and compares very well to the X-ray crystallographic structure of a related peptidyl inhibitor complexed to the enzyme. The fact that ligands such as MK **2** exist in solution in the bioactive conformation accounts, in part, for the observed inhibitory activity of activated ketone inhibitors bearing comparable peptidyl sequences. Comparison of the X-ray structures of HCMV protease apoenzyme and that of its complex with a related peptidyl α-ketoamide inhibitor allowed for a detailed analysis of the previously reported conformational change of the enzyme upon complexation of inhibitors such as **1** and **3**. The above observations indicate that HCMV protease is a novel example of a serine protease that operates by an induced-fit mechanism for which complexation of peptidyl ligands results in structural changes which bring the enzyme to a catalytically active (or optimized) form. Kinetic and fluorescence studies are also consistent with an induced-fit mechanism in which a considerable proportion of the intrinsic ligand-binding energy is used to carry out the conformational reorganization of the protease. Issues related to the rational design of both mechanism- and nonmechanism-based inhibitors of HCMV protease, notably in light of the peptidyl ligand-induced optimization of its catalytic functioning, are discussed.

## Introduction

Serine proteases are perhaps the most well-understood family of enzymes to date[1,2] whose study has played a very large role in furthering our comprehension of the functioning of enzymes in general. Much effort is presently being directed toward a particular group of serine proteases, the herpesvirus proteases (or assemblins), whose activity is essential for proper assembly of the capsid[3] and, as a consequence, viral replication.[4] It is therefore not surprising that a great deal of attention is being paid to these enzymes as therapeutic targets for the development of novel antiherpetic agents.[5,6] This is notably the case of the highly prevalent human cytomegalovirus (HCMV),[7] for which existing antiviral treatments suffer from toxicity and limited effectiveness.[8]

The quest for new inhibitors of HCMV protease has been paralleled by much activity focusing on the structural biology of the target, which has underlined the highly novel nature of this enzyme. X-ray crystallographic studies[9,10] have revealed HCMV protease to possess a protein fold previously unseen among serine proteases as well as a unique catalytic triad in

* To whom correspondence should be addressed. Phone: (450) 682-4640. Fax: (450) 682-8434.

† Present address: Department of Biological Sciences, Columbia University, New York, New York 10027.

(1) Polgar, L., Ed. *Mechanisms of Protease Action*; CRC Press: Roca Baton, FL, 1989.

(2) Fersht, A. *Enzyme Structure and Mechanism*, 2nd ed.; W. H. Freeman: New York, NY, 1985.

(3) Trus, B. L.; Booy, F. P.; Newcomb, W. W.; Brown, J. C.; Homa, F. L.; Thomsen, D. R.; Steven, A. C. *J. Mol. Biol.* **1996**, *263*, 447—462. Newcomb, W. W.; Homa, F. L.; Thomsen, D. R.; Booy, F. P.; Trus, B. L.; Steven, A. C.; Spencer, J. V.; Brown, J. C. *J. Mol. Biol.* **1996**, *263*, 447—462.

(4) Gao, M.; Matusick-Kumar, L.; Hurlburt, W.; DiTusa, S. F.; Newcomb, W. W.; Brown, J. C.; McCann, P. J., III; Deckman, I.; Colonno, R. J. *J. Virol.* **1994**, *68*, 3702—3712. Matusick-Kumar, L.; McCann, P. J., III; Robertson, B. J.; Newcomb, W. W.; Brown, J. C.; Gao, M. *J. Virol.* **1995**, *69*, 7113—7121.

(5) Howerda, B. C. *Antiviral Res.* **1997**, *35*, 1—21.

(6) Gibson, W.; Welch, A. R.; Hall, M. R. T. *Perspect. Drug Discov. Des.* **1994**, *2*, 413—426.

(7) Mocarski, E. S., Jr. In *Virology*; Fields, B. N., Ed.; Lippencott-Raven: Philadelphia, PA, 1995; Vol. 2, pp 2447—2492. Britt, W. J.; Alford, C. A. In *Virology*; Fields, B. N., Ed.; Lippencott-Raven: Philadelphia, PA, 1995; Vol. 2, pp 2493—2525.

(8) Goodgame, R. W. *Ann. Intern. Med.* **1993**, *119*, 924—935.

(9) Tong, L.; Qian, C.; Massariol, M.-J.; Bonneau, P.; Cordingley, M.; Lagacé, L. *Nature* **1996**, *383*, 272—275.

(10) Qiu, X.; Culp, J. S.; DiLella, A. G.; Hellmig, B.; Hoog, S. S.; Janson, C. A.; Smith, W. W.; Abdel-Meguid, S. S. *Nature* **1996**, *383*, 275—279. Shieh, H.-S.; Kurumball, R. G.; Stevens, A. M.; Stegeman, R. A.; Sturman, E. J.; Pak, J. Y.; Wittwer, A. J.; Palmier, M. O.; Wiegand, R. C.; Holwerda, B. C.; Stallings, W. C. *Nature* **1996**, *383*, 279—282. Chen. P.; Tsuge, H.; Almassy, R. J.; Gribskov, C. L.; Katoh, S.; Vanderpool, D. L.; Margosiak, S. A.; Pinko, C.; Kan, C.-C. *Cell* **1996**, *86*, 835—843.
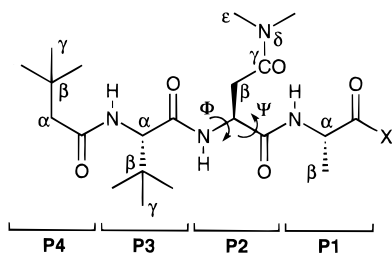
**Figure 1.** Nomenclature used in this study.

**Table 1.** Peptidyl Methyl and Activated Ketone Inhibitors of HCMV Protease

| Inhibitor[a] | IC$_{50}$ (µM) |
| --- | --- |



| | |
| --- | --- |
| **1:** R = CH$_3$　X = CH$_3$ | 2100 |
| **2:** R = H　　X = CH$_3$ | 5000 |
| **3:** R = CH$_3$　X = CF$_3$ | 1.1 |
| **4:** R = CH$_3$　X = CF$_2$CF$_3$ | 0.1 |
| **5:** R = CH$_3$　X = (O=C–N(H)–CH$_2$–Ph) | 0.2 |

[a] Compounds **3**, **4**, and **5** are epimerized at the P1 α-center.

which the third member is a histidine residue. Confirming biophysical studies, the enzyme has also revealed itself to exist as a dimer that is believed to be the sole active form.[11] We have recently provided spectroscopic evidence that the protease is an induced-fit enzyme, undergoing a conformational change upon complexation of substrate-based peptidyl inhibitors.[12]

In our efforts to develop potent inhibitors of HCMV protease, a large number of substrate-based, activated peptidyl ketones were synthesized.[13] Among the most active were those bearing a *tert*-butylacetyl-L-*tert*-butylglycyl-L-dimethylasparagyl-L-alanyl sequence (which mimics the P4-P1[14] Val-Val-Asn-Ala sequence of the natural Maturational (M-) cleavage site) flanking the activated carbonyl center (Figure 1). The IC$_{50}$ values, in the high nanomolar range, of these molecules are provided in Table 1. As part of our efforts to obtain a detailed understanding of the workings of HCMV protease and the structural basis of its inhibition by the above-mentioned compounds, we looked to NMR[15] and, in particular, the transferred nuclear Overhauser effect (TRNOE) experiment as a tool of choice.[16] This powerful NMR technique utilizes the rapid reversible binding of a ligand in solution to a macromolecule to obtain information concerning

the conformation of the former in the complexed state. We recently described such studies involving both M- and R-site sequence N-terminal cleavage products of HCMV protease.[17] In the present work, we provide details of our elucidation of an NMR structure of methyl ketone **2**, a probe that was designed to conform to the kinetic constraints of the TRNOE method. A combination of NMR methods were also employed to determine the conformational properties of MK **2** and related compounds in solution. These studies revealed that the predominant solution conformation of ketone **2** is very similar to that when complexed to HCMV protease, a property that is undoubtedly key to the observed binding of the optimized peptidyl sequence.

The recent disclosure[18] of the X-ray crystallographic structure of the related α-ketoamide inhibitor **18** complexed to HCMV protease allowed for comparison of enzyme-bound inhibitor structures derived by NMR and X-ray diffraction. Perhaps more importantly, it also permitted us to compare the structures of the free and inhibited protease and define the ligand-induced conformational changes. These analyses of both E[19] and I led us to conclude that HCMV protease is a unique example of a serine protease that clearly operates by an induced-fit mechanism. Consistent with this, kinetic studies indicate that factors (such as salt) which stabilize forms of the enzyme which approach the catalytically activated species reduce the proportion of the intrinsic binding energy used to effect the conformational change, resulting in stronger complexation of peptidyl ligands. The implications of these factors in the design of inhibitors, both mechanism- and non-mechanism-based, are addressed.

## Results and Discussion

**Design and Synthesis of Peptidyl Methyl Ketones. (a) Design of Noncovalent Peptidyl Ketone Inhibitors.** Peptidyl activated carbonyl compounds[20] represent a very large class of substrate-based serine protease inhibitors comprised of a peptidic chain and an electrophilic keto-functionality replacing the carbonyl group of the scissile peptide bond. Examples include trifluoromethyl ketones[21-23] (TFMKs), pentafluoroethyl ketones[24] (PFEKs), and α-ketoamides,[25] and among the many enzymes inhibited by this class of molecules, their action against chymotrypsin,[22,26] elastase,[27] and thrombin[28] has been most studied. The generally accepted mechanism of competitive inhibition is depicted in Figure 2 with the example of a peptidyl

(11) Margosiak, S. A.; Vanderpool, D. L.; Sisson, W.; Pinko, C.; Kan, C.-C. *Biochemistry* **1996**, *35*, 5300−5307. Darke, P. L.; Cole, J. L.; Waxman, L.; Hall, D. L.; Sardana, M. K.; Kuo, L. C. *J. Biol. Chem.* **1996**, *271*, 7445−7449.

(12) Bonneau, P. R.; Grand-Maître, C.; Greenwood, D. J.; Lagacé, L.; LaPlante, S. R.; Massariol, M.-J.; Ogilvie, W. W.; O'Meara, J. A.; Kawai, S. H. *Biochemistry* **1997**, *36*, 12644−12652.

(13) Ogilvie, W.; Bailey, M.; Poupart, M.-A.; Abraham, A.; Bhavsar, A.; Bonneau, P.; Bordeleau, J.; Chabot, C.; Duceppe, J.-S.; Fazal, G.; Goulet, S.; Grand-Maitre, C.; Guse, I.; Halmos, T.; Lavallée, P.; Leach, M.; Malenfant, E.; O'Meara, J.; Plante, R.; Plouffe, C.; Poirier, M.; Soucy, F.; Yoakim, C.; Déziel, R. *J. Med. Chem.* **1997**, *40*, 4113−4135.

(14) The peptide/peptidyl inhibitor and subsite nomenclature used is that of: Schechter, I.; Berger, A. *Biochem. Biophys. Res. Commun.* **1967**, *27*, 157−162.

(15) Wüthrich, K. *NMR of Proteins and Nucleic Acids*; John Wiley & Sons: New York, NY, 1986. Lian, L. Y.; Barsukov, I. L.; Sutcliffe, M. J.; Sze, K. H.; Roberts, G. C. K. *Methods Enzymol.* **1994**, *239*, 657−700.

(16) Ni, F. *Prog. Nucl. Magn. Reson.* **1994**, *26*, 517−590.

(17) LaPlante, S. R.; Aubry, N.; Bonneau, P. R.; Cameron, D. R.; Lagacé, L.; Massariol, M.-J.; Montpetit, H.; Plouffe, C.; Kawai, S. H.; Fulton, B. D.; Chen, Z. G.; Ni, F. *Biochemistry* **1998**, *37*, 9793−9801.

(18) Tong, L.; Qian, C.; Massariol, M.-J.; Déziel, R.; Yoakim, C.; Lagacé, L. *Nature Struct. Biol.* **1998**, *5*, 819−826.

(19) The following abbreviations are used throughout the text: E, enzyme; I, inhibitor; S, substrate; ES, Michaelis complex; EP, enzyme−product complex; E:I, enzyme−inhibitor complex.

(20) Mehdi, S. *Bioorg. Chem.* **1993**, *21*, 249−259.

(21) Imperiali, B.; Abeles, R. H. *Biochemistry* **1986**, *25*, 3760−3767. Peet, N. P.; Burkhart, J. P.; Angelastro, M. R.; Giroux, E. L.; Mehdi, S.; Bey, P.; Kolb, M.; Neises, B.; Schirlin, D. *J. Med. Chem.* **1990**, *33*, 394−407.

(22) Brady, K.; Abeles, R. H. *Biochemistry* **1990**, *29*, 7608−7617.

(23) Xeï, C. V. *Biochemistry* **1997**, *36*, 1308−1313.

(24) Angelastro, M. R.; Baugh, L. E.; Bey, P.; Burkhart, J. P.; Chen, T.-M.; Durham, S. L.; Hare, C. M.; Huber, E. W.; Janusz, M. J.; Koehl, J. R.; Marquart, A. L.; Mehdi, S.; Peet, N. P. *J. Med. Chem.* **1994**, *37*, 4538−4554.

(25) Hu, L.-Y.; Abeles, R. H. *Arch. Biochem. Biophys.* **1990**, *281*, 271−274. Brady, S. F.; Sisko, J. T.; Stauffer, K. J.; Colton, C. D.; Qiu, H.; Lewis, S. D.; Ng, A. S.; Shafer, J. A.; Bogusky, M. J.; Veber, D. F.; Nutt, R. F. *Bioorg. Med. Chem.* **1995**, *3*, 1063−1078.

(26) Liang, T.-C.; Abeles, R. H. *Biochemistry* **1987**, *26*, 7603−7608.

(27) Edwards, P. D.; Bernstein, P. R. *Medicinal Res. Rev.* **1994**, *14*, 127−194.

(28) Jones, D. M.; Atrash, B.; Ryder, H.; Teger-Nilsson, A.-C.; Gyzander, E.; Szelke, M. *J. Enzyme Inhib.* **1995**, *9*, 43−60.
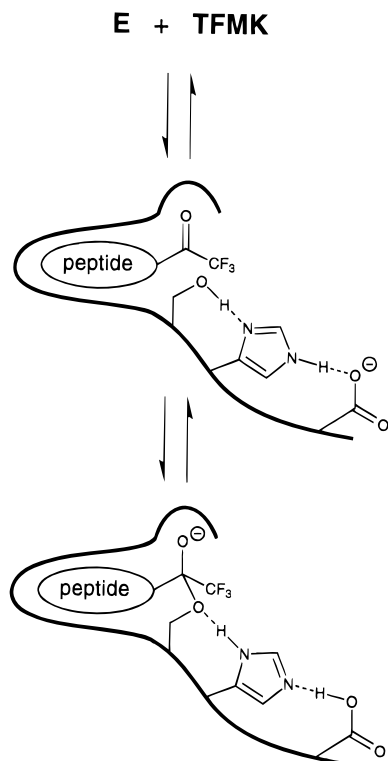
**E + TFMK**



**Figure 2.** Inhibition of a serine protease by a peptidyl trifluoromethyl ketone.

TFMK. Following the formation of an initial encounter complex (analogous to the Michaelis complex), attack of the active site serine hydroxyl on the reactive carbonyl center results in a covalent hemiketal adduct which, by virtue of the electron-withdrawing CF₃ substituent and its resemblance to the transition state, has an appreciable lifetime.

While the transferred nuclear Overhauser effect (TRNOE) method is clearly an expedient route to obtaining the bound conformation of a protein-complexed ligand, a key constraint of the technique is that the reversible exchange between the free and bound inhibitor be rapid enough to allow for cross relaxation. While activated carbonyl compounds such as **3**, **4**, and **5** are reversible inhibitors, the exchange rates between their free and enzyme-bound states are very slow due to their mechanism of inactivation of the enzyme (covalent modification), confering low $k_{off}$ rates (typically $7 \times 10^{-5}$ s$^{-1}$ for a peptidyl TFMK inhibitor of the present enzyme). Moreover, in the case of trifluoromethyl and pentafluoroethyl ketones, the high degree of hydration in the free state results in "slow-binding" kinetics.[29] As a consequence, TRNOE methods cannot be employed to determine the bound conformation of these inhibitors.

To circumvent the kinetic constraints of the TRNOE method, we sought to design a ligand that as closely as possible resembled our more potent inhibitors while not exhibiting its slow exchange properties. The peptidyl methyl ketones **1** and **2** clearly fulfill these criteria. Although close structural analogues of TFMK **3**, they are not hydrated in aqueous solution and do not form hemiketal adducts with the active site serine of HCMV protease. This latter conclusion is based on our NMR studies involving ¹³C carbonyl-labeled **1** which clearly demonstrated its unreactivity toward attack by the active site serine.[12] Another

(29) Stein, R. L.; Strimpler, A. M.; Edwards, P. D.; Lewis, J. J.; Mauger, R. C.; Schwartz, J. A.; Stein, M. M.; Trainor, D. A.; Wildonger, R. A.; Zottola, M. A. *Biochemistry* **1987**, *26*, 2682–2689. Brady, K.; Abeles, R. H. *Biochemistry* **1990**, *29*, 7608–7617.

**Scheme 1.** Synthesis of Peptidyl Methyl Ketones **1** and **2**
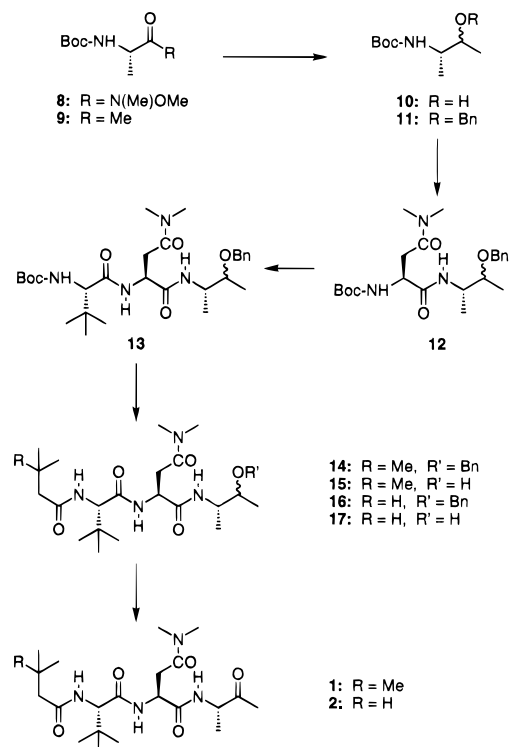


feature of the present methyl ketones is the presence of the ketonic CH₃ group that gives rise to an additional NMR resonance which could potentially provide further distance information to aid definition of the conformation in the P1-P1′ region.

**(b) Synthesis of Methyl Ketone Inhibitors 1 and 2.** Although a number of methods have been reported for the transformation of α-amino acids and peptides to their equivalent methyl ketones,[30] the problems of epimerization at the α-carbon and/or unsatisfactory yields prompted us to investigate Weinreb methodgy[31] (Scheme 1). Indeed, the alanyl ketone **9** could be obtained from *N*-Boc-alanine via reaction of its Weinreb amide **8** with excess methyllithium in 94% yield, and which proceeded without any detectable racemization of the α-center. Ketone **9** was then reduced with borohydride to a mixture of diastereomeric alcohols **10** which were subsequently protected by benzylation to give **11**. Attempted peptide coupling of either ketone **9** or amino alcohols **10** following *N*-deprotection proved unsatisfactory.

Standard peptide coupling employing 1-hydroxybenzotriazole (HOBT) and 1-(3-dimethylaminopropyl)-3-ethylcarbodiimide hydrochloride (EDAC) was then used to elongate the peptide chain from compounds **11**, each step proceeding in very good yield (86–94%). The coupling of the P2 dimethylasparagine unit was carried out at 0 °C to reduce the epimerization we observed in related work. Quantitative removal of the benzyl groups of **14** and **16** by hydrogenation over palladium, followed by Dess–Martin oxidation of the resultant alcohols, afforded the target peptidyl methyl ketones **1** and **2**, respectively.

**NMR Studies. (a) Conformation of Free Peptidyl Ligands.** In contrast to proteins, small peptides are generally viewed as

(30) Thompson, R. C. *Biochemistry* **1974**, *13*, 5495–5501. Mansour, T. S.; Evans, C. A. *Syn. Commun.* **1989**, *19*, 667–672. Klix, R. C.; Chamberlin, S. A.; Bhatia, A. V.; Davis, D. A.; Hayes, T. K.; Rojas, F. G.; Koops, R. W. *Tetrahedron Lett.* **1995**, *36*, 1791–1794. McMurray, J. S.; Dyckes, D. F. *J. Org. Chem.* **1985**, *50*, 1112–1115. Myers, A. G.; Yoon, T. *Tetrahedron Lett.* **1995**, *36*, 9429–9432.

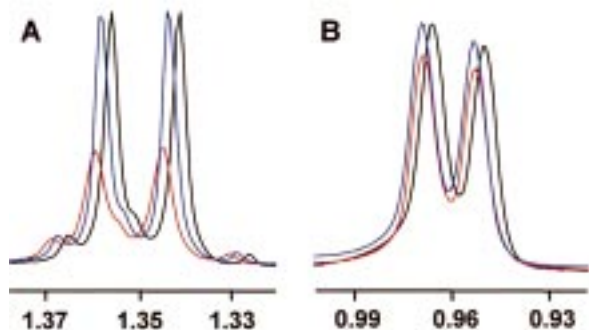(31) Nahm, S.; Weinreb, S. M. *Tetrahedron Lett.* **1981**, *22*, 3815–1818.

**Figure 3.** (A) Effect of HCMV protease on the P1-$\beta$CH$_3$ doublet of MK **1** (400 MHz): (blue) 2 mM MK **2**, (red) after the addition of protease (**2**:protease = 7:1), and (black) after the subsequent addition of PFEK **4** (2 equiv with respect to protease). (B) Effect of HCMV protease on the P4-$\gamma$CH$_3$ doublet of MK **2** (400 MHz): (blue) 3.3 mM **2**, (red) after the addition of protease (**2**:protease = 10:1), (black) after subsequent addition of $\beta$-lactam **23** (2 equiv with respect to protease; see Table 5 for structure). Black traces have been displaced for the sake of clarity.
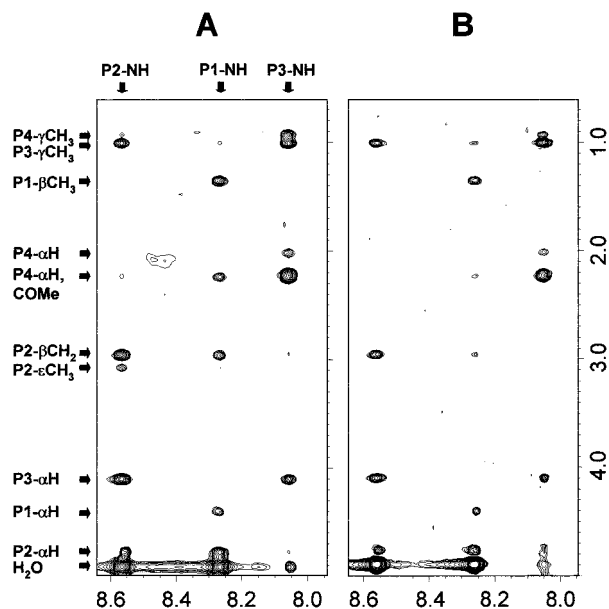


**Figure 4.** Comparison of 2D spectra of free versus bound MK **2** (all experiments carried out in aqueous buffer/750 MHz/283 K/3.1 mM **2**): (A) NH-aliphatic region of the transferred NOESY spectrum in the presence of HCMV protease (**2**:protease = 7:1/150 ms mixing time), (B) ROESY spectrum in the absence of protease (125 ms spin-lock mixing time).

being devoid of defined structure in aqueous solution, their NMR data representing an average of all of the solution conformations present. Nonetheless, it has been demonstrated through a combination of NMR techniques that certain short peptide chains do exist predominantly in one particular conformation.[32] The solution structure of peptidyl ketone **2** was investigated through rotating-frame NOE (ROESY) methods. The NH-aliphatic region of the 2D spectrum is shown in Figure 4B and indicates that the molecule is indeed structured. A clear feature of the ROESY data is a characteristic pattern of weak intramolecular [C$^{\alpha}$H(*i*)-NH(*i*)] correlations alternating with intense interresidue [C$^{\alpha}$H(*i*)-NH(*i* + 1)] signals. This, together with the absence of any cross-peaks between adjacent NH protons, indicates that

(32) Dyson, H. J.; Cross, K. J.; Houghten, R. A.; Wilson, I. A.; Wright, P. E.; Lerner, R. A. *Nature* **1985**, *318*, 480−483. Dyson, H. J.; Rance, M.; Houghten, R. A.; Lerner, R. A.; Wright, P. E. *J. Mol. Biol.* **1988**, *201*, 161−200.

**Table 2.** Substitutions of the P3 Side Chain of Pentafluoroethyl Ketone Inhibitors

| Inhibitor | IC$_{50}$ ($\mu$M) |
|---|---|
|  | |
| **4:** R = C(CH$_3$)$_3$ | 0.1 |
| **6:** R = CH$_3$ | 48 |
| **7:** R = H | >300 |

**Table 3.** $^1$H Chemical Shift and Coupling Constant Data for Inhibitors **1**, **2**, **4**, **6**, and **7** in H$_2$O/DMSO$^a$

| | proton | MK (**1**) | MK (**2**) | PFEK (**4**) | PFEK (**6**) | PFEK (**7**) |
|---|---|---|---|---|---|---|
| | | | chemical shift (ppm) | | | |
| P1 | NH | 7.96 | 7.95 | 7.42 | 7.43 | 7.58 |
| | COCH$_3$ | 2.03 | 2.03 | | | |
| | $\alpha$-H | 4.11 | 4.11 | 4.13 | 4.14 | 4.15 |
| | $\beta$-CH$_3$ | 1.13 | 1.13 | 1.04 | 1.05 | 1.07 |
| P2 | NH | 8.17 | 8.19 | 8.21 | 7.99 | 7.98 |
| | $\alpha$-H | 4.56 | 4.56 | 4.52 | 4.52 | 4.55 |
| | $\beta$-CH$_2$ | 2.65/2.72 | 2.65/2.72 | 2.63/2.70 | 2.62/2.71 | 2.61/2.71 |
| | $\epsilon$-CH$_3$ | 2.76/2.92 | 2.76/2.92 | 2.75/2.90 | 2.77/2.91 | 2.71/2.91 |
| P3 | NH | 7.61 | 7.74 | 7.63 | 8.02 | 8.15 |
| | $\alpha$-H | 4.04 | 4.06 | 4.07 | 4.14 | 3.62/3.66 |
| | $\beta$-CH$_3$ | | | | 1.16 | |
| | $\gamma$-CH$_3$ | 0.88 | 0.87 | 0.86 | | |
| P4 | $\alpha$-H$_A$ | 2.00 | 2.01 | 1.98 | 1.96 | 1.98 |
| | $\alpha$-H$_B$ | 2.15 | 2.10 | 2.14 | 1.99 | 2.01 |
| | $\beta$-CH | | 1.91 | | | |
| | $\gamma$-CH$_3$ | 0.91 | 0.83 | 0.90 | 0.91 | 0.91 |
| | | | $^3J_{(H)-(H)}$ Coupling Constant (Hz) | | | |
| P1 | NH-$\alpha$-H | 6.2 | 6.7 | 9.3 | 9.3 | 9.3 |
| | $\alpha$-H-$\beta$-H | 7.2 | 7.2 | 6.8 | 6.7 | 6.8 |
| P2 | NH-$\alpha$-H | 7.7 | 7.7 | 7.6 | 7.9 | 7.9 |
| | $\alpha$-H-$\beta$-H$_A$ | 6.1 | 6.1 | 7 | 6.5 | 6 |
| | $\alpha$-H-$\beta$-H$_B$ | 6.1 | 6.1 | 6.1 | 5.6 | 6 |
| P3 | NH-$\alpha$-H | 8.2 | 8.2 | 8.6 | 7.0 | 5.8/5.8 |

$^a$ Values reported for the hydrated forms of inhibitors **4**, **6**, and **7**.

MK **2** exists predominantly in an extended peptide conformation. In addition, a weak but detectable correlation between the P2 side chain and N-terminal isopropyl methyl groups (data not shown) is consistent with a certain population existing such that the P4 group is oriented toward the same side of the peptide backbone as the P2 side chain.

Selected proton NMR parameters for methyl ketones **1** and **2** are listed in Table 3 and, as one would expect, consist of two very similar sets of values. Of particular interest are the magnitudes of $^3J_{NH-\alpha H}$. Consistent with the conformational picture derived from the ROESY data, the coupling constants for P2 and P3 indicate a predominantly extended peptide structure. The values also compare well to those obtained for the PFEK analogue of methyl ketone **1** (compound **4**). The difference in the case of P1 is no doubt related to the fact that the activated pentafluoroethyl ketones are sterically congested due to hydration whereas the methyl ketones **1** and **2** are not. We ascribe the smaller coupling constants to substantial contributions by nonextended conformers.

The fact that compounds bearing the peptidyl sequence of **1** exist predominantly as extended structures is underlined by comparing their conformational properties with analogues lacking the bulky side chain at the P3 position for which one would predict a much greater degree of flexibility in solution. A series of NMR experiments, performed in 15% H$_2$O in DMSO-$d_6$ for reasons of solubility, were carried out for the

**Table 4.**  $^{13}$C Chemical Shift and $NT_1$ Values of PFEK Inhibitors **4**, **6**, and **7** in H$_2$O/DMSO$^a$

| | carbon | PFEK (4) $\delta$ (ppm) | $NT_1$ (s) | PFEK (6) $\delta$ (ppm) | $NT_1$ (s) | PFEK (7) $\delta$ (ppm) | $NT_1$ (s) |
|---|---|---|---|---|---|---|---|
| P1 | $\alpha$-CH | 48.78 | 0.30 | 48.78 | 0.3$^b$ | 48.64 | 0.3$^b$ |
| | $\beta$-CH$_3$ | 15.37 | 1.74 | 15.01 | 1.74 | 14.82 | 1.62 |
| P2 | $\alpha$-CH | 50.27 | 0.29 | 49.82 | 0.32 | 49.50 | 0.30 |
| | $\beta$-CH$_2$ | 34.48 | 0.38 | 34.87 | 0.46 | 34.81 | n.d. |
| | $\gamma$-C=O | 170.30 | 1.65 | 170.13 | 1.73 | 169.77 | 1.85 |
| | $\epsilon$-CH$_3$ | 35.51/37.32 | 2.34/2.76 | 35.30/37.15 | 2.12/3.00 | 34.98/36.80 | 2.74/3.08 |
| | C=O | 170.92 | 1.04 | 170.88 | 1.20 | 170.74 | 1.04 |
| P3 | $\alpha$-CH | 60.96 | 0.33 | 48.64 | 0.37 | 42.29 | 0.50 |
| | $\beta$-C | 34.24 | 2.69 | 17.96 | 2.46 | | |
| | $\gamma$-CH$_3$ | 27.09 | 2.61 | | | | |
| | C=O | 171.29 | 0.94 | 172.83 | 1.02 | 169.20 | 1.22 |
| P4 | $\alpha$-CH$_2$ | 48.78 | 0.58 | 48.78 | 0.7$^b$ | 48.64 | 0.9$^b$ |
| | $\beta$-C | 31.15 | 4.39 | 30.88 | 4.90 | 30.51 | 5.07 |
| | $\gamma$-CH$_3$ | 30.16 | 3.69 | 29.96 | 4.50 | 29.64 | 4.77 |
| | C=O | 172.54 | 1.02 | 172.33 | 1.31 | 172.28 | 1.47 |

$^a$ $N$ = number of attached hydrogens, $T_1$ = longitudinal relaxation time. Values reported for the hydrated forms of the inhibitors. In the case of carbonyl and quaternary carbons, $T_1$ values are given. $^b$ Estimated values (see Supporting Information). The direct measurement of $T_1$ was precluded by the overlap of the P1 and P4 signals.

series of pentafluoroethyl ketones **4**, **6**, and **7** (Table 2). The ROESY spectrum of compound **4** (data not shown) was, not surprisingly, similar to that of MK **2** in aqueous solution, being consistent with an extended backbone conformation. Comparison of the ROESY spectra of inhibitors **6** and **7** revealed marked differences upon the reduction of the steric bulk at P3. Most notable was a sharp decrease in the relative intensities of particular cross-peaks, notably the volumes of the interresidue NH–C$\alpha$H correlations. In the cases of the P1–NH to P2-$\alpha$H, P2-NH to P3-$\alpha$H, and P3-NH to P4-$\alpha$CH$_2$ cross-peaks, the relative signal volumes measured for inhibitors **6** and **7** with respect to those of compound **4** were 74 and 70%, 47 and 56% (two protons), and 57 and 48%, respectively. Globally, the comparative analysis of the ROESY spectra argue strongly for the view that the peptidyl chains of **1**, **2**, and **4** are fairly rigid extended structures and that these conformational properties are maintained to a considerable degree by the P3 *tert*-butyl substituent.

Selected coupling constants and chemical shifts for the PFEKs are also listed in Table 3. These values correspond to the hydrated forms of the inhibitors which predominate in solution. The $^3J_{\text{NH}-\alpha\text{H}}$ value for P3 is also consistent with an extended conformation for **4** (8.6 Hz). We interpret the value of 7.0 Hz for inhibitor **6** as being due to a certain contribution by nonextended populations. In contrast, the values of 5.8 for the P3-Gly-substituted inhibitor **7** point to a freely rotating $\phi$ bond. The chemical shift data, in particular the $\alpha$-CH$_2$ signals of the N-terminal acyl group, also reveal differences within the series of PFEKs. Whereas the shifts of the diastereotopic protons are very similar ($\Delta\delta$ = 0.03 ppm) for molecules **6** and **7**, they are separated by 0.16 ppm in the case of inhibitor **4**, indicating that the two exist in distinct magnetic environments and suggesting that rotation about the $\psi$ bond is much more restricted in the latter, the terminal acyl group having a preferred orientation.

Finally, carbon-13 $T_1$ values of the three compounds were measured to further evaluate the dynamic properties of the compounds (Table 4). $NT_1$ values (the product of the number of attached protons and the longitudinal relaxation time) provide information concerning the mobility of a molecule[33] in solution and have been used to investigate the conformational dynamics of peptidic compounds.[34] Examination of the $NT_1$ values of the $\alpha$-carbons of PFEK **4** reveals little segmental motion along P1

to P3 with a higher degree of mobility for the P4 *tert*-butylacetyl group. Removal of steric bulk at the P3 position results in an overall increase in the $NT_1$ values for all of the carbon atoms from the P3-residue onward and, notably, for the N-terminal acyl moiety. As one would expect, this rise in conformational freedom is most pronounced for the P3-glycyl-substituted compound **7**.

**(b) Protease-Bound Conformation of MK 2.**[35] Our initial studies toward the determination of the bound conformation of the present peptidyl methyl ketones focused on clearly establishing that they indeed bind to the active site of HCMV protease in a specific fashion. Upon addition of the enzyme to aqueous samples of MK **1**, uniformly broadened proton resonances of the ketone were observed. These changes in peak form were dependent on the protein/ligand ratio, indicative of rapid reversible complexation to the protease. The specific nature of the binding was verified by the addition of the potent and slow-exchanging PFEK inhibitor **4**, which resulted in elimination of line-broadening in the MK signals (Figure 3A). In fact, the disappearance of the enzyme-induced line-broadening of MK **1** resonances, due to its displacement from the protease by a more potent competitive inhibitor, was later used to investigate the action of nonpeptidic inhibitors of HCMV protease. Figure 3B presents the results of such a study involving the $\beta$-lactam **23**, and demonstrates that this inhibitor acts by blocking access to the active site. Analogous 2D competition experiments were also carried out (data provided in the Supporting Information). Numerous negative correlations in the NOESY spectrum of MK **1** in the presence of HCMV protease were found to disappear upon the addition of PFEK **4**, providing unequivocal evidence that the binding of the methyl ketone is specific in nature.

While many of the initial NMR experiments were carried out for MK **1**, it was evident that the overlap of the two *tert*-butyl singlets in its proton spectrum would limit the information that could be provided. It was in considering this fact that TRNOE studies were carried out for the P4 isopropylacetyl inhibitor **2** for which this unfortuitous signal overlap is not present. Since the intensities (volumes) of TRNOE cross-peaks are proportional to interproton distances ($\propto r^{-6}$), they provide valuable distance information concerning the conformation of

(33) Lyerla, J. R., Jr.; Levy, G. C. *Top. Carbon-13 NMR Spectrosc.* **1974**, *1*, 79–148.

(34) Kessler, H.; Bats, J. W.; Griesinger, C.; Koll, S.; Will, M.; Wagner, K. *J. Am. Chem. Soc.* **1988**, *110*, 1033–1049.

(35) Preliminary communication: LaPlante, S. R.; Cameron, D. R.; Aubry, N.; Bonneau, P. R.; Déziel, R.; Grand-Maître, C.; Ogilvie, W. W.; Kawai, S. H. *Angew. Chem., Int. Ed. Engl.* **1998**, *37*, 2729–2732.
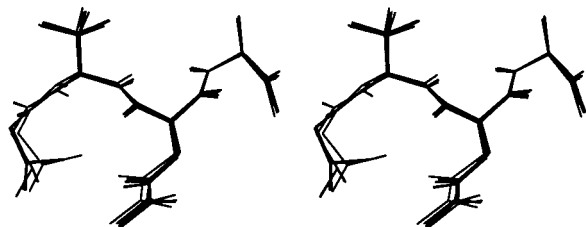
**Figure 5.** Family of NMR-derived bound structures of MK **2**. Twenty-nine overlapping conformations are shown in stereoview.

a macromolecule-bound ligand. In the presence of HCMV protease, the NOESY spectrum of a 12-fold excess of MK **2** presented numerous negative correlations. The volumes of the signals were scaled and converted to interproton distance restraints[36] with use of the P1-$\alpha$H to P1-$\beta$CH$_3$ cross-peak to correlate volumes with distances. Twenty-nine low-energy, TRNOE-derived structures were generated by restrained simulated annealing and are shown in Figure 5.

**(c) Comparison of Free and Bound Structures of MK 2.** The investigations of the solution structure of MK **2** led to the conclusion that the peptide is relatively structured, existing predominantly in an extended conformation with the somewhat mobile N-terminal acyl group oriented, at least part of the time, toward the same side of the backbone as the P2 side chain. This conformation corresponds very well to the NMR-derived enzyme-bound structure of the ligand as presented in Figure 5. The similarity between the protease-bound conformations of MK **2** and its solution structure is also clearly evidenced by comparison of the ROESY spectrum of the free ligand and its transferred NOESY spectrum in the presence of HCMV protease. The corresponding NH-aliphatic regions of the two traces are presented in Figure 4 to underline the similarity of cross-relaxation within the free and protease-bound systems. A more quantitative comparison of the normalized cross-peak volumes (Supporting Information) emphasizes the very similar backbone conformations as well as the fact that the N-terminal product **20** is also bound in the same fashion.

Of equal interest is the appearance or, more importantly, the increase in the relative intensities of certain NH to side-chain signals in the TRNOE spectrum relative to the ROESY trace. Globally, this is a result of the immobilization of certain groups which exhibit a certain mobility in solution (e.g., P2 side chain and ketonic methyl groups) and whose ROESY signals are not observed. Other peaks are weaker due to the fact that only a certain proportion of the molecules are present in the bioactive conformation (not excluding the possibility of contributions from other orientations). The fact that certain signals, such as the P3-NH to P4-$\gamma$CH$_3$ and P3-NH to P4-$\beta$CH$_2$ correlations, are present in the ROESY spectrum is consistent with a nonnegligible population of MK **2** existing in solution with the same side-chain orientation as when protease bound.

On the basis of these comparisons, we conclude that MK **2** exists predominantly in the bioactive conformation when free in solution, notably with respect to its backbone geometry, and that complexation by HCMV protease occurs with very little conformational adjustment within the ligand. This is certainly the case as well for the much more potent activated carbonyl analogues of MK **2** which bear essentially identical peptidyl chains (i.e., inhibitors **3**, **4**, and **5**).

**(d) Comparison of NMR and X-ray Structures.** We recently reported TRNOE studies involving HCMV protease N-terminal cleavage products.[17] The NMR-derived bound

structure of the R-site product **20** was determined to be an extended peptide. As one would anticipate, comparison with the present structures generated for MK **2** (Figure 6) reveals that the two families of conformations overlap very well, confirming that substrate and inhibitor bind in the same mode. Figure 7 also includes the structure of protease-complexed $\alpha$-ketoamide **18** taken from the X-ray structure of the inhibited enzyme.[18] Again, the extended peptide structures overlap well from the P4 to P2 residues. The differences at P1 likely stem from the fact that ketoamide **18** exists as the covalent adduct with the active site serine whereas MK **2** is not a covalent inhibitor and may interact differently with the enzyme in the region of the catalytic serine and oxyanion hole.

It is clear, therefore, that the present activated peptidyl inhibitors undergo little change in conformation between the free and covalently linked states. This point is of importance since it strongly implies that very little adjustment of the bound inhibitor occurs over the course of the reorganization of the protease upon inhibitor binding (see below). Otherwise, one could question whether the NMR-derived structures presented in Figure 5 represent the pre- or post-conformational change structure of MK **2**, or a virtual structure. TRNOE studies involving ligands which themselves undergo conformational exchange concurrent with complexation[37] can be problematic and necessitate the application of particular methods for the proper handling of transferred NOESY data.[38] This, however, does not appear to be the case for the present system.

**Mechanism of Inhibition. (a) Ligand-Induced Structural Changes in HCMV Protease.** Our previous fluorescence and circular dichroism studies demonstrated that HCMV protease undergoes a conformational change upon complexation of inhibitors **1**, **3**, **4**, and **5**.[12] A key observation to come out of these investigations was that formation of a covalent adduct between E and I is not required to induce the structural alterations which are no doubt elicited by the formation of contacts between the peptidyl portion of the inhibitors and binding regions in the active site. Comparison of the X-ray structures of HCMV protease apoenzyme[9] and its covalent complex with ketoamide **18**[18] allows for a structural analysis of this conformational transition.

Many enzymes bear flexible surface loops which have been observed in either of two conformations depending on whether a ligand is present.[39,40] These structures are believed to play a role in forming the binding-pocket for the substrate and/or be indirectly implicated in catalysis. In many cases, these loops are "lid-hinges"[40] of which a large portion is a rigid structure that moves about a flexible joint. The conformational change in HCMV protease is a much more complex process, involving the movement and rigidification of a relatively large portion of the active site region as shown in Figures 7 and 8.

The X-ray structure of HCMV protease inhibited by ketoamide **18** revealed that the peptidyl portion of the ligand is bound primarily through formation of an antiparallel $\beta$-sheet with the $\beta$5-strand of the enzyme, a key interaction being between P3 and Ser-135. In the apoenzyme, this strand, which bears the catalytic Ser-132, is more or less disordered from Ser-134

(36) Baleja, J. D.; Moult, J.; Sykes, B. D. *J. Magn. Res. B* **1990**, *87*, 375−384.

(37) Nicotra, M.; Paci, M.; Sette, M.; Oakley, A. J.; Parker, M. W.; Lo Bello, M.; Caccuri, A. M.; Federici, G.; Ricci, G. *Biochemistry* **1998**, *37*, 3020−3027.

(38) Moseley, H. N. B.; Curto, E. V.; Krishna, N. R. *J. Magn. Res. B* **1995**, *108*, 243−261.

(39) Derewenda, U.; Brzozowski, A. M.; Lawson, D. M.; Derewenda, Z. S. *Biochemistry* **1992**, *31*, 1532−1541. Jia, Z.; Barford, D.; Flint, A. J.; Tonks, N. K. *Science* **1995**, *268*, 1754−1758. Wlodawer, A.; Erickson, J. W. *Annu. Rev. Biochem.* **1993**, *62*, 543−585.

(40) Joseph, D.; Petsko, G. A.; Karplus, M. *Science* **1990**, *249*, 1425−1428.

**Figure 6.** Comparison (stereoview) of NMR-derived bound conformations of MK **2** (green; 29 structures), R-peptide **20** (gray; 32 structures), and the X-ray crystallographic structure of bound ketoamide **18** (yellow; 4 conformations).
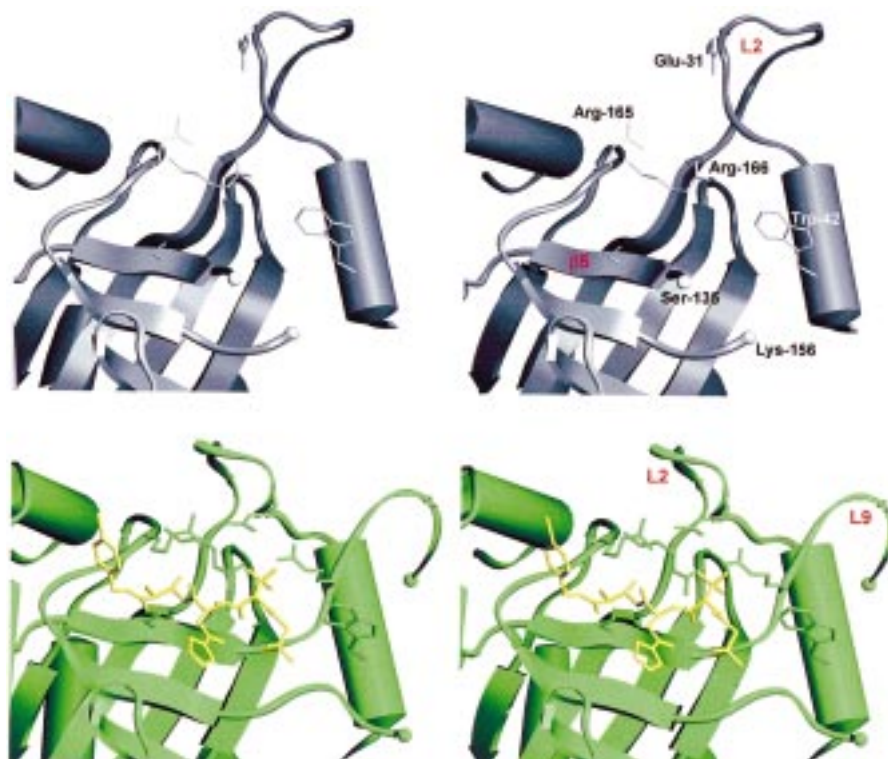


**Figure 7.** Peptidyl ligand-induced conformational change of HCMV protease. Stereoviews of the active site region of the apoenzyme (above, in gray) and of the inhibited enzyme (below, in green) covalently modified by ketoamide **18** (see Table 5 for chemical structure) shown in yellow. Spheres indicate the points at which the L9-loop was no longer resolved. For the sake of clarity, single representative structures of the apoenzyme (out of two) and of the complex (out of four) are presented. This applies as well to Figure 8.

through the L9 loop which is not resolved until Lys-156. After superimposing the apoenzyme and inhibited protease structures, the extent of the changes which occur upon ligand binding was revealed and may be summarized as follows: (a) movement and ordering of the $\beta$5-strand; (b) ordering of the L9-loop and a large change in the position of the L2-loop such that a cleft in which the P1 and P3 side chains find themselves is formed (this involves formation of a putative double-salt bridge between Arg-137, Glu-31, and Arg-165); and (c) repositioning of Arg-165 and Arg-166. These residues constitute the oxyanion hole whose structure is also altered upon ligand binding. Thus, HCMV protease undergoes a substantial reorganization and, notably, rigidification upon peptidyl ligand binding. It should also be noted that the inhibitor-induced changes in the L9-loop result in burying and immobilization of Trp-42, which in the free enzyme is, more or less, solvent exposed and clearly mobile. This change in microenvironment is responsible for the reported shifts in fluorescence emission upon peptidyl ligand binding.[12] A number of other structural alterations occur which have been described[18] and are of lesser importance in the present context.

While X-ray crystallography may provide "snapshots" of discrete states (i.e., apoenzyme and enzyme−ligand complex) in a crystal lattice which allows for the identification of ligand-induced alterations in protein structure, the exact manner by which these changes occur is not revealed.[41] It must be emphasized that viewing the conformational change observed for HCMV protease as consisting of a well-defined transition between discreet structures is a gross oversimplification. It is clear that the free enzyme in solution exists as an ensemble of a great many, rapidly interconverting structures, and that the complexation of a rigid peptidyl ligand results, above all, in a restriction of the flexibility of the protein. In this respect, the process bears elements of protein conformer selection.[42] However, we believe that this partial immobilization[43] of the active site region can only occur once a ligand is bound. In other

(41) For a review covering the conformational adaptability of enzymes, see:  Citri, N. *Adv. Enzymol.* **1973**, *37*, 397−649.

(42) Cao, Y.; Musah, R. A.; Wilcox, S. K.; Goodin, D. B.; McRee, D. E. *Protein Sci.* **1998**, *7*, 72−78.

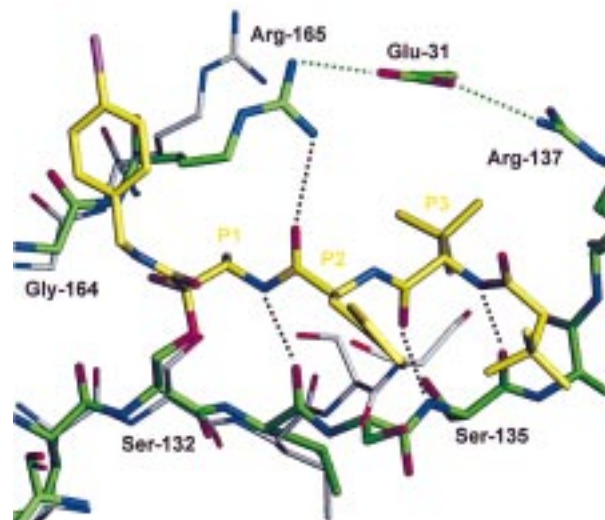(43) Davis, J. H.; Agard, D. A. *Biochemistry* **1998**, *37*, 7696−7707.

**Figure 8.** Peptidyl ligand-induced conformational change of HCMV protease showing the alterations in the $\beta$5-strand and the oxyanion hole. The Arg-Glu-Arg double salt bridge is also shown (same color scheme as for Figure 7; iodine is shown in pink).

words, the peptide guides the reorganization of the protein around it after initial association.

**(b) Inhibition of HCMV Protease by Peptidyl Activated Carbonyl Compounds.** Having analyzed the conformational properties of both free and enzyme-bound inhibitors bearing the peptide sequence of MKs **1** and **2**, and after examination of the changes in protein structure upon ligand binding by the protease, we believe that the inhibition of HCMV by analogous activated carbonyl compounds proceeds as follows: (a) An encounter complex forms between the flexible apo-form(s) of E and I, the latter existing as a relatively fixed and extended peptide structure; (b) formation of the H-bonds between I and the $\beta$5-strand of E in the active site, notably those involving the P3 residue, results in the above-described structural reorganization and rigidification of the protease, which brings E to its active or optimal catalytic form; and (c) after the conformational change, the active site is properly organized for formation of the hemiketal adduct, which can strongly interact with the active site owing to its structural similarity to the tetrahedral intermediate (or, more precisely, the transition state of its formation or breakdown) of the catalytic reaction.[44]

**(c) HCMV Protease As an Induced-Fit[45] Enzyme.** While the X-ray crystallographic comparisons and fluorescence studies provide very convincing evidence as to the induced-fit character of HCMV protease, truly unequivocal proof was provided by observation of the conformational change during substrate hydrolysis. By fluorescence, the peptidyl ligand-induced structural change manifests itself as a blue shift of 5−7 nm in the emission maximum of the enzyme upon specific tryptophan excitation.[12] (See Figure 9A for the spectral change due to the binding of PFEK **4**.) Figure 9B compares the fluorescence spectra of the enzyme alone and in the presence of the nonfluorogenic substrate **21** at an initial concentration far above its $K_M$ and at approximately 50% conversion to product (i.e., enzyme saturation). A blue-shift similar to that observed in the presence of peptidic inhibitors can clearly be seen.

The induced-fit mechanism also accounts for other biophysical properties of the enzyme. The marked activating effect of salts on the catalytic efficiency of herpes proteases is well established[46,47] and, in the case of HSV-1 protease, has been
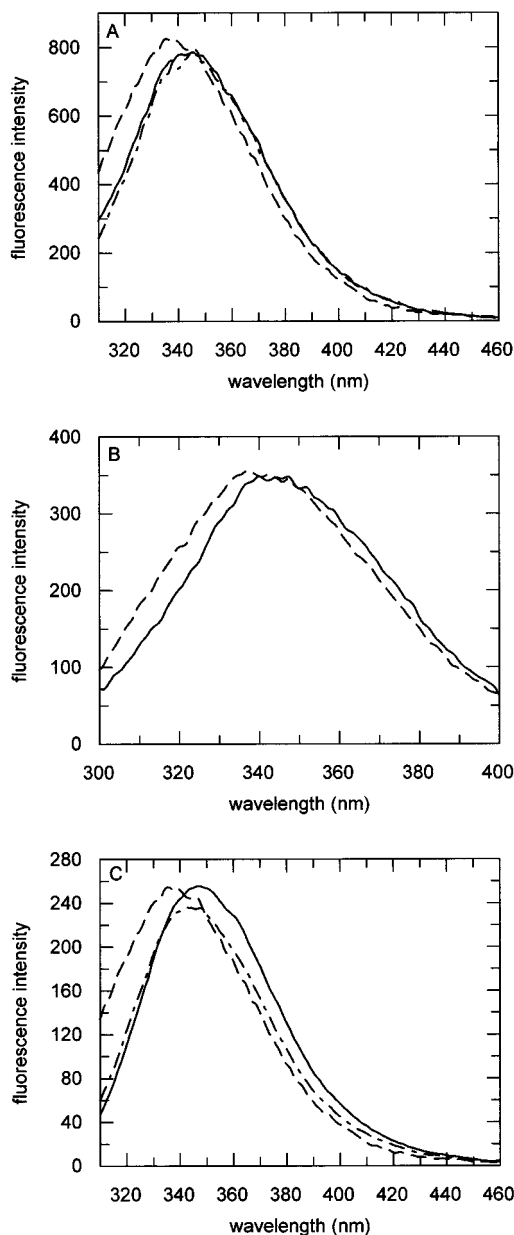


**Figure 9.** Effect of ligand binding and Na$_2$SO$_4$ on the fluorescence emission spectrum of HCMV protease. All spectra were acquired after tryptophan excitation at 280 nm. (A) The effect of inhibitor binding: HCMV protease alone (−) and in the presence of saturating concentrations of PFEK **4** (- - -) and $\beta$-lactam **24** (−·−). The trace for **24** was scaled to facilitate comparison with that of the free enzyme. The decrease in fluorescence upon binding of **24** is ascribed to absorption of excitation energy by the aromatic groups of the inhibitor. (B) The effect of substrate binding: HCMV protease alone (−) and in the presence of a 30-fold excess of the nonfluorogenic substrate **21** after 50% conversion (- - -). (C) The effect of sodium sulfate: HCMV protease alone in buffer (−) and after the addition of Na$_2$SO$_4$ to a concentration of 0.5 M (−·−). The emission spectrum of the enzyme saturated with PFEK **4** in the presence of 0.5 M Na$_2$SO$_4$ (- - -).

correlated to a blue-shift in the emission spectrum of the enzyme. While similar salt activation has been observed for HCMV
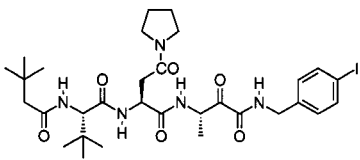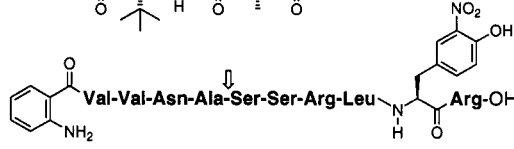
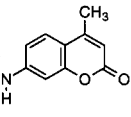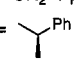(44) Mader, M. M.; Bartlett, P. A. *Chem. Rev.* **1997**, *97*, 1281−1301.
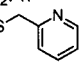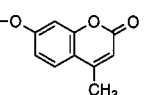
(45) Koshland, D. E., Jr. *Proc. Natl. Acad. Sci. U.S.A.* **1958**, *44*, 98−104. Jencks, W. P. *Adv. Enzymol.* **1975**, *43*, 219−410.

(46) Hall, D. L.; Darke, P. L. *J. Biol. Chem.* **1995**, *270*, 22697−22700.

(47) Yamanaka, G.; DiIanni, C. L.; O'Boyle, D. R., II; Stevens, J.; Weinheimer, S. P.; Deckman, I. C.; Matusick-Kumar, L.; Colonno, R. J. *J. Biol. Chem.* **1995**, *270*, 30168−30172.

**Table 5.**  Structures of Other Substrates/Inhibitors Referred to in This Work

| Inhibitor or Substrate[a] | IC$_{50}$ ($\mu$M) | Ref. |
|---|---|---|
| **18:** | 0.3 | 18 |
| **19:** | – | 64 |
| **20:** Thr-Glu-Arg-Glu-Ser-Tyr-Val-Lys-Ala-OH | – | 17 |
| **21:** Ac-**Tbg-Tbg-Asn(Me$_2$)**-Ala-Ser-Ser-Arg-Leu-Ala-OH | – | – |
| **22:** Ac-**Tbg-Tbg-Asn(Me$_2$)-Ala** | – | 64 |
| **23:** R = CH$_2$-4-pyridyl; R' = H; X = CH$_2$Ph | 12 | 59 |
| **24:** R = Ph; R' = H; X = –S–CH$_2$-pyridyl | 0.5 | 60 |
| **25:** R = CH$_2$-4-pyridyl; R' = Me; X = –O– coumarin | 0.6 | 63 |



[a] Abbreviations of unnatural amino acids:  Tbg = *tert*-butylglycine, Asn(Me$_2$) = $N^\delta,N^\delta$-dimethylasparagine.

**Table 6.**  Kinetic Parameters for the Hydrolysis of Peptide Substrate (**22**) Under Varying Salt Conditions[a]

|  | no salt | 0.5 M Na$_2$SO$_4$ | 1.5 M NaCl |
|---|---|---|---|
| $k_{cat}$, s$^{-1}$ | 0.052 | 0.19 | 0.17 |
| $K_M$, $\mu$M | 132 | 6.5 | 31 |
| $k_{cat}/K_M$, M$^{-1}$ s$^{-1}$ | 390 | 30000 | 5400 |

[a] Values listed represent the averages from two experiments. Both salt conditions are of the same ionic strength (1.5 M).

protease,[47,48] no detailed studies have been reported. Figure 9C presents the effect of Na$_2$SO$_4$ on the fluorescence emission of the present enzyme. A blue-shift in the emission maximum upon the addition of sulfate is evident. Kinetic studies were subsequently performed under identical buffer conditions to determine the effect of Na$_2$SO$_4$ on the kinetic parameters for the hydrolysis of the optimized substrate **22** (Table 6). The results clearly indicate that the 75-fold increase in catalytic efficiency between 0 and 0.5 M sodium sulfate is due, in very large part, to a marked drop (20-fold) in $K_M$.

These results are clearly consistent with the induced-fit model for HCMV protease. According to Fersht,[49] induced fit mediates against catalysis by increasing $K_M$ for all substrates according to the equation:

$$K_{M(obs)} = K_M^*/K$$

where $K$ = [E*]/[E$_{unact}$] in the absence of S, and E* is the activated enzyme form following the conformational change.[50]

(48) Burke, P. J.; Berg, D. H.; Luk, T. P.; Sassmannshausen, L. M.; Wakulchik, M.; Smith, D. P.; Hsiung, H. M.; Becker, G. W.; Gibson, W.; Villarreal, E. C. *J. Virol.* **1994**, *68*, 2937–2946.

**Scheme 2.**  Mechanism of Induced-Fit Catalysis Incorporating the Partially Activated Enzyme Species E′
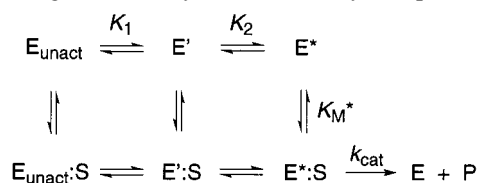


In other words, the strength of binding of the substrate is reduced by a factor ($K$) that reflects the energy cost of converting the enzyme (conformational change) to its activated form E*. The presence of sulfate, however, should not be looked upon as shifting the equilibrium $K$ toward E* but, rather, as introducing an intermediate species E′ that approaches the activated enzyme as depicted in Scheme 2. Thus, $K$ is broken into two equilibrium constants ($K = K_1K_2$) such that part of the free energy cost of

(49) For the derivation of this equation based on the scheme below, see ref 2 (pp 332–333). $K_M^*$ (treated as a simple dissociation constant) may be viewed as the $K_M$ for a lock-and-key enzyme that always exists in the activated form E*. Although the induced-fit reaction proceeds via E$_{unact}$:S, the value $K_{M(obs)}$ also represents the global dissociation constant for E*:S $\rightleftharpoons$ E$_{unact}$ + S proceeding via E*.
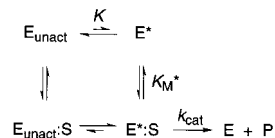


(50) $K$ is the equilibrium constant for the hypothetical conformational equilibrium between unactivated (E$_{unact}$) and activated (E*) forms of the free enzyme in solution. In reality, E* only exists when substrate is bound.
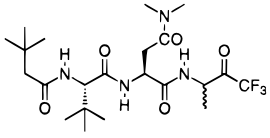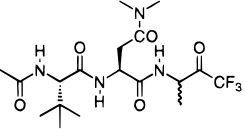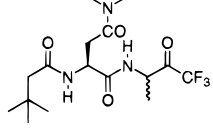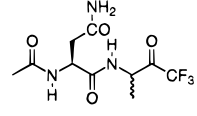
*Characterization of the Human Cytomegalovirus Protease*

*J. Am. Chem. Soc., Vol. 121, No. 13, 1999* 2983

converting $E_{unact}$:S to E*:S, which is normally paid for by the free energy of ligand binding in the absence of salt, is provided for by the presence of sulfate such that $K_{M(obs)salt} = K_M*/K_2$.

From the values provided in Table 6, one can calculate[51] $K_1$ to be 0.05, which corresponds to 1.8 kcal/mol of free energy available for substrate binding in the presence of 0.5 M sulfate which would otherwise have been spent in effecting the change in enzyme conformation in the absence of the salt. Thus, the sequential blue-shifts in the fluorescence of HCMV protease as shown in Figure 9C are due to conversion of $E_{unact}$ to E′ (or more precisely a mixture of $E_{unact}$ and the various species constituting E′) by sulfate, and then to E*−I upon the binding of the peptidyl ligand. It is likely that unstructured regions of the protease which are critical for ligand binding ($\beta$5-strand, L9-loop) acquire a certain preorganization in the presence of kosmotropic agents such as sulfate which would decrease the entropic loss when they are rigidified upon ligand complexation. Table 6 also lists the kinetic parameters in the presence of sodium chloride, again indicating an increase, albeit smaller, in the specificity constant and consistent with the observed salt activation of HSV-1 protease.[46,47]

The induced-fit nature of HCMV protease is another of the many characteristics setting it apart from classical serine proteases which are generally acknowledged to be "lock-and-key"[52] enzymes based on high-resolution X-ray crystallographic studies. The description of the functioning of HCMV protease outlined above bears some similarity to the workings of certain aspartic proteases[53] for which P3-S3 interaction alters the active site such that $k_{cat}$ is increased without changing $K_M$. In the case of elastase, a large increase in $k_{cat}/K_M$ (due, principally, to an increase in $k_{cat}$) upon the addition of a P3-residue to shorter substrates has led to the proposal[54] that it is an induced-fit enzyme for which P3-S3 interaction engages the catalytic triad. In the present case, the inherently low catalytic activity of HCMV protease has precluded this type of kinetic investigation. However, truncation studies of TFMK inhibitors (Table 7) showed that sequential removal of groups from the C-terminal end of TFMK **3** results in substantial drops in inhibitory activity. We attribute these decreases in potency, at least in part, to the removal of key features of the inhibitors which are required by the protease to optimally form the covalent adduct.

Examination of the structure of HCMV protease inhibited by **18** reveals that the molecule lies on the surface of the protein and that the side chains which are not solvent exposed (P1 and P3) are buried upon changes in enzyme structure which are triggered by ligand binding. There are no highly defined pockets which one would expect to confer a high degree of substrate specificity due to steric complementarity. The description of ligand binding we outline above fits well in the context of the natural enzyme reaction. The induced-fit recognition of a particular backbone conformation may be, in part, the mechanism by which HCMV protease achieves a certain selectivity. Considering the polyvalent function of HCMV protease and the fact that the target sequence within the assembly protein precursor is likely held in a rigid manner on a supramolecular

**Table 7.** Truncation of Trifluoromethyl Ketone **3**



| Inhibitor | IC$_{50}$ ($\mu$M) |
| --- | --- |
| **3:** | 1.1 |
| **26:** | 2.8 |
| **27:** | 57 |
| **28:**[a] | >300 |

[a] The dimethylasparagine analogue of **28** is also expected to have an IC$_{50}$ value of well over 300 $\mu$M based on the modest increase in potency observed for the change in other series.

protein scaffold, it is perhaps logical that evolution select a protease possessing a certain flexibility to accommodate the binding of such immobilized recognition sequences. As discussed above, the low turnover rate for the enzyme compared to digestive serine proteases is consistent with the induced-fit mechanism that mediates against catalysis. The observed kinetic properties of the protease may be linked to its function in the infected cell, being tuned to the relatively slow capsid assembly process.[55] Furthermore, the kinetic activation by salts, which is again related to induced fit, may be a reflection of the behavior of the protease when it finds itself in the particular micro-environment of the nucleus or within the capsid.[46,47]

**Inhibitor Design. (a) Peptidyl Inhibitors.** The obvious question arises as to how one could possibly increase the potency of the present peptidyl activated carbonyl inhibitors. The dissociation constant of the complex formed between an ideal transition-state analogue ($K_{TX}$) and enzyme target is related to the rate acceleration observed for the enzymatic reaction with respect to the uncatalyzed rate:[56]

$$K_{TX} = k_{uncat}/(k_{cat}/K_M)$$

For dipeptidyl TFMK inhibitors of chymotrypsin, $K_i$ values of approximately 3 orders of magnitude more than the calculated $K_{TX}$ value of 0.5 pM were measured, leading to the conclusion that about 65% of the potential transition-state binding is made use of.[22] In the case of HCMV protease, the $K_{TX}$ value based on the kinetic parameters for the hydrolysis of substrates bearing the optimized P4-P1 sequence present in **1** is in the $10^{-15}$ to $10^{-14}$ M range.[57] Thus, inhibitors **3** to **5** remain far from exploiting all of the binding available for transition-state stabilization.

(51) $K_{M(obs)salt}/K_{M(obs)no\ salt} = (K_M*/K_2)/(K_M*/K_1\ K_2) = K_1$.
(52) Fischer, E. *Chem. Ber.* **1894**, *27*, 2985−2993.
(53) Sali, A.; Veerapandian, B.; Cooper, J. B.; Moss, D. S.; Hofmann, T.; Blundell, T. L. *Proteins: Struct. Funct. Genet.* **1992**, *12*, 158−170.
(54) Stein, R. L.; Strimpler, A. M.; Edwards, P. D.; Lewis, J. J.; Mauger, R. C.; Schwartz, J. A.; Stein, M. M.; Trainer, D. A.; Wildonger, R. A.; Zottola, M. A. *Biochemistry* **1997**, *26*, 22682−2689. Stein, M. A.; Hori, H.; Powers, J. C. *Biochemistry* **1987**, *26*, 1301−1305. Stein, R. L.; Strimpler, A. M.; Hori, H.; Powers, J. C. *Biochemistry* **1987**, *26*, 1305−1314.

(55) Babé, L. M.; Craik, C. S. *Cell* **1997**, *91*, 427−430.
(56) Wolfenden, R. *Acc. Chem. Res.* **1972**, *5*, 10−18. Wolfenden, R. *Annu. Rev. Biophys.* **1976**, *5*, 271−306.
(57) Based on a $k_{uncat}$ for amide hydrolysis of $10^{-11}$ s$^{-1}$ (Yamana, T.; Mizukami, Y.; Tsuji, A.; Yasuda, Y.; Masuda, K. *Chem. Pharm Bull.* **1972**, *20*, 881−891).

The factors contributing to the inhibitory activity of TFMK **3** and related analogues can be, therefore, dissected as follows: (i) *The rigidified elongated peptidyl chain bearing amide groups properly disposed to H-bond with the β5-strand.* The NMR studies described above clearly demonstrate that inhibitors such as **2** and **4** possess a fair degree of structure in solution that corresponds to the conformation when bound to HCMV protease, effectively reducing the loss of conformational entropy upon complexation. It appears that the presence of the bulky side chains stabilizes the bioactive backbone conformation, the P3 *tert*-butyl substituent playing a key role. The measured $\phi$ angles for the peptidyl chain of protease-bound **18** in the X-ray structure were used to calculate[58] the theoretical magnitudes of $^3J_{NH-\alpha H}$ for the bioactive conformation. The values for P1 to P3 were determined to be 9.5, 9.2, and 8.2 Hz, respectively. Comparison of these values to those in Table 3 is consistent with our analysis that, for MK **2**, P3 is locked in the optimal conformation and that other nonextended conformers contribute to the observed *J* values for P2 and P1.

It is clear that the binding of the peptidyl portion of the present ketone inhibitors is not very strong as evidenced by the poor inhibition by MKs **1** and **2** which are not transition-state analogues. Moreover, we have observed that the 1D proton NMR resonances of covalently enzyme-bound TFMK inhibitors remain surprisingly sharp (data not shown). This would indicate that, even as hemiketal adducts, the present peptidyl inhibitors retain a high degree of mobility with respect to the protein and that the E:I interactions, notably those involving the inhibitor side chains, are probably quite weak.

(ii) *The electrophilic carbonyl which allows for formation of a stabilized hemiketal that mimics the transition state.* Formation of the covalent adduct that, owing to its structural analogy with the catalytic transition-state, may interact strongly with the enzyme is the key factor contributing to inhibitor potency. This is clearly demonstrated by the >1000-fold increase in potency in proceeding from MK **1** to TFMK **3**. One might, therefore, expect the strongest effects on activity being observed upon changes to the activated carbonyl moiety.

Thus, the inhibition of HCMV protease by TFMK **3** and related activated carbonyl compounds involves the synergistic effect of a peptidyl portion required to induce the transition to a catalytically active or activated form of the enzyme, and an electrophilic keto moiety that may then react to yield a stabilized covalent complex mimicking the transition-state. This accounts for the relatively weak binding of the peptidyl chain and is consistent with the view that, in induced-fit catalysis, binding energy is expended to compensate for the energy required to convert the enzyme to a thermodynamically less favorable state. In view of the magnitude of the observed alterations in protein structure, notably the apparent ordering of otherwise random regions, one would anticipate a very large and unfavorable entropic factor associated with E*:I complex formation.

**(b) β-Lactam Inhibitors.** It has been suggested that molecules which complex to, but do not induce the conformational change associated with an induced-fit enzyme would be better suited as inhibitors since free energy of binding is not utilized to effect the structural change in the macromolecule.[53] Such molecules would be expected to exhibit binding constants reflecting, more directly, the structural interactions between ligand and protein. In fact, medicinal chemistry efforts later focused on a class of inhibitors, the β-lactams,[59-62] which inhibited HCMV protease by binding to the active site without

inducing the structural reorganization as observed by fluorescence emission (Figure 9A). The blue-shift normally observed upon the binding of peptidyl inhibitors or substrate (as reported above) was not produced upon saturation of the enzyme with β-lactam inhibitors such as compound **24**, the spectrum remaining essentially identical with that of the free enzyme.

Detailed mechanistic studies have shown these molecules to be very slowly cleaved competitive substrates of HCMV protease for which an acylated form of a nonactivated enzyme may accumulate.[63] Comparison of the kinetic parameters for the hydrolysis of the substrate **19** and those of the β-lactam probe **25** is telling. In the case of peptide cleavage, respective $k_{cat}$ and $K_M$ values of 0.2 s$^{-1}$ and 760 $\mu$M were measured,[64] figures which agree with those reported in the literature for comparable substrates.[5] In the case of β-lactam hydrolysis, the respective $k_{cat}$ and $K_M$ values were found to be 0.00043 s$^{-1}$ and 0.6 $\mu$M.[63] Such differences, namely increased binding coupled to lowered catalytic efficiency, are exactly what one would anticipate for an inhibitor that does not elicit the protease-activating conformational change. The degree to which the form of the enzyme acting on a β-lactam substrate is far from one optimized for catalysis is further underlined in considering the slow hydrolysis of the acyl-enzyme ($k_{deacylation}$ being the rate-determining step at 0.00043 s$^{-1}$), being 500-fold slower than the $k_{cat}$ for peptide hydrolysis. Such a large discrepancy is what one would anticipate for the induced-fit mechanism. Therefore, the inhibitory activity of β-lactams such as **25** is owed, in part, to the fact that their sub-optimal processing by the protease occurs at such a slow rate.

## Conclusion

Through the use of a number of NMR methods, we have demonstrated that inhibitors such as **1−5** of HCMV protease exist as fairly rigid, extended structures in solution and that the bulky P3 *tert*-butyl side chain is strongly implicated in maintaining this conformation. Moreover, the structure of the free ligand, as exemplified by MK **2**, is very similar to that when complexed to the enzyme as determined by TRNOE and X-ray crystallographic methods. This fact undoubtedly contributes to a significant degree to the observed inhibitory activity. Comparison of the X-ray structures of the free and inhibited protease revealed the changes in protein structure which occur upon ligand binding. Combined, the information allows us to propose a mechanism of induced-fit inhibition (and catalysis) for this novel serine protease.

From an enzymological viewpoint, the characterization of HCMV protease as an induced-fit enzyme represents a significant observation. This is especially so by virtue of the fact that it is a serine protease for which many members of the family are among the best characterized enzymes to date. Since classical serine proteases such as chymotrypsin operate through a lock-

(58) Pardi, A.; Billeter, M.; Wüthrich, K. *J. Mol. Biol.* **1984**, *180*, 741−751.

(59) Yoakim, C.; Ogilvie, W. W.; Cameron, D. R.; Chabot, C.; Guse, I.; Haché, B.; Naud, J.; O'Meara, J. A.; Plante, R.; Déziel, R. *J. Med. Chem.* **1998**, *41*, 2882−2891.

(60) Déziel, R.; Malenfant, E. *Bioorg. Med. Chem. Lett.* **1998**, *8*, 1437−1442.

(61) Yoakim, C.; Ogilvie, W. W.; Cameron, D. R.; Chabot, C.; Grand-Maître, C.; Guse, I.; Haché, B.; Kawai, S. H.; Naud, J.; O'Meara, J. A.; Plante, R.; Déziel, R. *Antiviral Chem. Chemother.* **1998**, *9*, 379−387.

(62) Borthwick, A. D.; Weingarten, G.; Haley, T. M.; Tomaszewski, M.; Wand, W.; Hu, Z.; Bédard, J.; Jin, H.; Yuen, L.; Mansour, T. S. *Bioorg. Med. Chem. Lett.* **1998**, *8*, 365−370.

(63) Bonneau, P. R.; Hasani, F.; Plouffe, C.; Malenfant, E.; LaPlante, S. R.; Guse, I.; Ogilvie, W. W.; Plante, R.; Davidson, W. C.; Hopkins, J. L.; Morelock, M. G.; Cordingley, M. G.; Déziel, R. **1999**, *121*, 2965−2973.

(64) Bonneau, P. R.; Plouffe, C.; Pelletier, A.; Wernic, D.; Poupart, M.-A. *Anal. Biochem.* **1998**, *255*, 59−65.

and-key mechanism, comparison with HCMV protease, which effects peptide cleavage through the same chemical steps, should further our understanding of the differences between lock-and-key and induced-fit models of catalysis. Detailed kinetic studies characterizing the present enzyme are clearly wanting and will no doubt aid in the development of new inhibitors.

From the perspective of drug design, our medicinal efforts constitute an interesting example of how two different classes of competitive inhibitors of comparable potency exercise their activity in two very different ways. In the case of the activated peptidyl ketones, inhibition relies on optimal functioning of the catalytic machinery. They are mechanism-based inhibitors which depend on complexation of their peptidic chains to bring the enzyme to an activated state, even though this interaction does not contribute to a great degree to the overall binding.

In the case of the $\beta$-lactam inhibitors, the intrinsic binding energy appears to be a much more important factor in endowing potency. Having made the comparison between the $K_M$ values for peptide and $\beta$-lactam hydrolysis above, it is perhaps more important to consider the differences in the dissociation constant, $K_S$ (i.e., for E:I $\rightleftharpoons$ E + I). In the case of peptidyl inhibitor MK **1**, $K_S = K_I = 2.1$ mM, whereas for the $\beta$-lactam **25**, the $K_S$ was determined to be 64 $\mu$M.[63] Thus, despite the much higher degree of noncovalent interaction between E and I for peptidyl inhibitors, the much smaller $\beta$-lactam binds greater than 30-times more tightly to the protease.

For these latter molecules, nonoptimized functioning of the catalytic machinery (i.e., the absence of induced-fit activation) is a key factor since it prevents rapid processing of the inhibitors which are also substrates for the enzyme. Interestingly, there is some evidence in the case of $\beta$-lactams lacking a heteroatom substituent at the C-4 position that the acylation rate may approach that for the deacylation of the protease. If this is so, the noncovalent E:I complex also accumulates and must be considered as well to be an inhibitory species. Therefore, the most advantageous strategy in inhibitor design may, perhaps, be a molecule that binds in the same mode as a $\beta$-lactam (i.e., no activating conformational change) but which is not at all prone to processing by the suboptimal form of the enzyme.

## Experimental Section

**Synthesis: General Methods.** NMR spectra were recorded on a Bruker AMX400 spectrometer and are referenced to internal tetramethylsilane. Peak multiplicities are denoted by the following abbreviations: app, apparent; br, broad; s, singlet; d, doublet; t, triplet; $q^4$, quartet; $q^5$, quintet; and m, multiplet (asterisk indicates overlapping signals). A reference value of 77.00 ppm was used for the $^{13}$C solvent signal of chloroform. The following abbreviations are used: TBG (*tert*-butylglycine), TBA (*tert*-butylacetyl), and IPA (isopropylacetyl). IR spectra were recorded on a Mattson Research Series spectrophotometer. FAB mass spectra (thioglycerol) were recorded on either Autospec VG or Kratos MS50 instruments (at the Department of Chemistry, Université de Montréal). Optical rotation measurements were carried out in a Perkin-Elmer 241 polarimeter. UV spectra were obtained with a Perkin-Elmer Lambda 7 UV/VIS instrument. Analytical HPLC employed either of the following systems: (A) Vydac C18 10 mm analytical column (24 × 4.6 mm), mobile phase: acetonitrile/0.06% trifluoroacetic acid (TFA) in water/0.06% TFA; (B) Symmetry shield C8 10 mm analytical column (15 × 3.9 mm), mobile phase: acetonitrile in 20 mM Na$_2$HPO$_4$, pH 9.0. Flash chromatography was performed on Merck silica gel 60 (0.040–0.063 mm) with nitrogen pressure. Analytical thin-layer chromatography (TLC) was carried out on precoated (0.25 mm) Merck silica gel F-254 plates. Anhydrous grade (Aldrich) dichloromethane and *N,N*-dimethylformamide were employed and tetrahydrofuran was distilled from lithium aluminum hydride immediately prior to use.

**(3*S*)-3-[(*tert*-Butoxycarbonyl)amino]butan-(2*R*,*S*)-2-ol Benzyl Ether (11).** Carbonyl diimidazole (23.0 g, 0.142 mol) was added to a stirred solution of *N*-Boc-alanine (20.0 g, 0.106 mol) in anhydrous dichloromethane (350 mL) cooled to 0 °C and the reaction was stirred under a nitrogen atmosphere. After 0.5 h, triethylamine (19.8 mL, 0.142 mol) and *N,O*-dimethylhydroxylamine hydrochloride (13.85 g, 0.142 mol) were added and the stirring at 0 °C was continued for 0.5 h after which time the reaction was allowed to warm to ambient temperature. After 14 h, the solution was poured into ethyl ether (800 mL) and the organic phase was washed with hydrochloric acid (1 N, 3 × 250 mL), saturated sodium bicarbonate (250 mL), and brine (250 mL). The ether phase was dried (MgSO$_4$), filtered, and evaporated in vacuo to yield Weinreb amide **8** (23.1 g, 94%) as a white solid that was used without further purification. $^1$H NMR (400 MHz, CDCl$_3$): $\delta$ 1.29 (d, 3H, $J = 7.0$ Hz, Ala-$\beta$-Me), 1.42 (s, 9H, *t*-Bu), 3.19 (s, 3H, NMe), 3.75 (s, 3H, OMe), 4.65 (br m, 1H, Ala-$\alpha$-H), 5.23 (br d, 1H, $J = 7.3$ Hz, NH). MS: *m/z* (rel intensity) 233 (MH$^+$, 92), 177 ([MH$^+$ − C$_4$H$_8$], 100), 133 ([MH$^+$ − Boc], 86), 91 (26), 57 (70).

Methyllithium (1 M in ethyl ether, 60.0 mL, 60.0 mmol) was added slowly to a stirred solution of Weinreb amide **8** (5.07 g, 21.8 mmol) in anhydrous tetrahydrofuran (230 mL) at −78 °C under a nitrogen atmosphere and the resulting solution was stirred for 1.5 h. The reaction was then quenched with saturated ammonium chloride (100 mL) and extracted with ethyl acetate (100 + 400 mL). The combined organic phases were washed with water (500 mL) and brine (500 mL) and then dried (MgSO$_4$), filtered, and evaporated in vacuo to yield methyl ketone **9** as a pale yellow oil (4.45 g, quantitative) that partially solidified upon standing and was used without further purification. $^1$H NMR (400 MHz, CDCl$_3$): $\delta$ 1.34 (d, 3H, $J = 7.3$ Hz, Ala-$\beta$-Me), 1.44 (s, 9H, *t*-Bu), 2.20 (s, 3H, C(O)Me), 4.30 (m, 1H, Ala-$\alpha$-H), 5.24 (br s, 1H, NH). MS: *m/z* (rel intensity) 188 (MH$^+$, 37%), 132 ([MH$^+$ − C$_4$H$_8$], 100), 91 (41), 88 ([MH$^+$ − Boc], 61), 57 (66).

Sodium borohydride (907 mg, 24.0 mmol) was added to a stirred solution of ketone **9** (4.09 g, 21.8 mmol) in tetrahydrofuran (42 mL) containing methanol (10 mL) at 0 °C and the reaction was stirred for 2 h. The solution was then diluted with ethyl ether (170 mL) and quenched by the slow addition of aqueous citric acid (10% w/v, 85 mL). The aqueous phase was extracted with ether (3 × 85 mL) and the combined organic phases were washed with saturated sodium bicarbonate (170 mL) and brine (170 mL), dried (MgSO$_4$), filtered, and evaporated in vacuo to yield the alcohols **10** (4.15 g, quantitative, mixture of diastereomers) as a white solid that was used without further purification. $^1$H NMR (400 MHz, CDCl$_3$): major isomer, $\delta$ 1.09 (d, 3H, $J = 7.0$ Hz, Ala-$\beta$-Me), 1.14 (d, 3H, $J = 6.4$ Hz, CH(OH)*Me*), 1.45 (s, 9H. *t*-Bu), 3.60 (br m, 1H, Ala-$\alpha$-H), 3.85 (dq$^4$, $J = 3.2$, 6.4 Hz, C*H*(OH)), 4.62* (br s, 1H, NH); minor isomer, $\delta$ 1.16 (d, 3H, $J = 7.0$ Hz, Ala-$\beta$-Me), 1.19 (d, 3H, $J = 6.4$ Hz, CH(OH)*Me*), 1.45 (s, 9H. *t*-Bu), 3.56 (br m, 1H, Ala-$\alpha$-H), 3.69 (dq$^4$, $J = 4.7$, 6.4 Hz, C*H*(OH)), 4.62* (br s, 1H, NH). MS: *m/z* (rel intensity) 280 (MH$^+$, 52%), 134 ([MH$^+$ − C$_4$H$_8$], 100), 90 ([MH$^+$ − Boc], 87), 57 (48).

The mixture of alcohols **10** (995 mg, 5.26 mmol) was added to a stirred suspension of sodium hydride (211 mg, 60% oil disp., 5.28 mmol) in dry *N,N*-dimethylformamide (14 mL) cooled to 0 °C followed by tetra-*n*-butylammonium iodide (97 mg, 0.26 mmol). After 0.5 h, benzyl bromide (0.75 mL, 6.31 mmol) was added and the reaction was allowed to warm to ambient temperature under a nitrogen atmosphere. After 1 day, the mixture was diluted with ethyl ether/ethyl acetate (1:1 v/v, 100 mL) and washed with water (50 mL), saturated sodium bicarbonate (50 mL), and brine (50 mL). The organic phase was then dried (MgSO$_4$), filtered, and evaporated in vacuo yielding an orange oil that was purified by flash chromatography (SiO$_2$, hexane/ethyl acetate = 6/1 to 4/1) to yield the benzyl ethers **11** (644 mg, 44%, mixture of diastereomers) as a colorless oil. $^1$H NMR (400 MHz, CDCl$_3$): major isomer, $\delta$ 1.12 (d, 3H, $J = 7.0$ Hz, Ala-$\beta$-Me), 1.16 (d, 3H, $J = 6.4$ Hz, CH(OR)*Me*), 1.43 (s, 9H, *t*-Bu), 3.56–3.64* (br m, 1H, C*H*(OR)), 3.66–3.77 (br m, 1H, Ala-$\alpha$-H), 4.44 and 4.62 (ABq$^4$, 2H, $J = 11.8$ Hz, C*H$_2$*Ph), 4.62* (br s, 1H, NH), 7.23–7.37* (m, 5H, Ph); minor isomer, $\delta$ 1.17 (d, 3H, $J = 6.7$ Hz, Ala-$\beta$-Me), 1.18 (d, 3H, $J = 6.4$ Hz, CH(OH)*Me*), 1.44 (s, 9H, *t*-Bu), 3.50 (dq$^4$, 1H, $J = 2.7$, 6.4 Hz, C*H*(OR)), 3.56–3.64* (br m, 1H, Ala-$\alpha$-H), 4.43 and 4.62 (ABq$^4$, 2H, $J = 11.8$ Hz, C*H$_2$*Ph), 4.62* (br s, 1H, NH), 7.23–7.37*

(m, 5H, Ph). MS: *m/z* (rel intensity) 280 (MH⁺, 37%), 224 ([MH⁺ − C₄H₈], 82), 180 ([MH⁺ − Boc], 46), 91 ([C₇H₇⁺], 100), 57 (27). HRMS (C₁₆H₂₆O₃N): calcd 280.1913; found 280.1922.

**(3S)-3-[N-tert-Butylacetyl-L-(α-tert-butylglycyl)-L-(Nᵟ,Nᵟ-dimethylasparagyl)amino]butan-2-one (1).** Alcohols **15** (200 mg, 0.452 mmol) were dissolved in anhydrous dichloromethane (10 mL) containing N,N-dimethylformamide (0.5 mL) and Dess−Martin periodinane (383 mg, 0.904 mmol) was added. After the mixture was stirred at ambient temperature for 2.5 h under a nitrogen atmosphere, the reaction was diluted with dichloromethane (10 mL) and a mixture of 10% sodium thiosulfate/saturated sodium bicarbonate (1:1 v/v, 50 mL) was added and the phases vigorously stirred. After 0.5 h, the clear phases were extracted with ethyl acetate (50 + 30 mL) and washed with saturated sodium bicarbonate (4 × 50 mL) and brine (50 mL). The combined organic phases were then dried (Na₂SO₄), filtered, and evaporated in vacuo to a colorless foam. The product was dissolved in boiling ethyl acetate and the solution was allowed to cool, resulting in the precipitation of a white solid. The material was filtered, washed with cold solvent, and dried under vacuum, affording methyl ketone **1** (112 mg, 56%) as a white powder. ¹H NMR (400 MHz, CDCl₃): δ 1.04 (s, 18H, 2 × t-Bu), 1.34 (d, 3H, J = 7.3 Hz, Ala-β-Me), 2.11 and 2.14 (ABq⁴, 2H, J = 13.0 Hz, TBA-α-H) 2.17 (s, 3H, C(O)Me), 2.50 (dd, 1H, J = 7.0, 16.5 Hz, Asn(Me₂)-β-Hₐ), 2.94 and 3.00 (two s, 2 × 3H, NMe₂), 3.13 (dd, 1H, J = 3.2, 16.5 Hz, Asn(Me₂)-β-H_B) 4.20 (d, 1H, J = 8.6 Hz, TBG-α-H), 4.46 (app q⁵, 1H, J_app = 7.3 Hz, Ala-α-H), 4.84 (app dt, 1H, J_app = 3.2, 7.3 Hz, Asn(Me₂)-α-H), 6.03 (d, 1H, J = 8.3 Hz, TBG-NH), 7.43 (d, 1H, J = 7.6 Hz, Asn(Me₂)-NH), 7.68 (d, 1H, J = 6.7 Hz, Ala-NH). ¹³C NMR (100.6 MHz, CDCl₃): δ 16.72, 26.29, 26.85, 29.86, 31.00, 34.30, 34.77, 35.53, 37.34, 49.38, 50.76, 54.99, 61.36, 170.45, 170.54, 171.04, 171.89, 206.59. MS: *m/z* (rel intensity) 441 (MH⁺, 100%), 354 ([MH⁺ − AlaMe], 11), 230 ([Asn-(Me₂)AlaMe + H⁺], 21), 212 (19), 184 (11), 115 (74). IR: 1713 cm⁻¹. [α]²²D +47.3° (c 0.516, CHCl₃). UV: λ_max = 282 nm (ε = 46, MeOH). HRMS (C₂₂H₄₁O₅N₄): calcd 441.3077; found 441.3112. HPLC: system A >99%, system B >99%.

**(3S)-3-[N-Isopropylacetyl-L-(α-tert-butylglycyl)-L-(Nᵟ,Nᵟ-dimethylasparagyl)amino]butan-2-one (2).** Alcohols **17** (161 mg) were oxidized as described above for the preparation of **1** above. The crude product was purified by flash chromatography (SiO₂, ethyl acetate/ ethanol = 10/1), which afforded methyl ketone **2** (112 mg, 70%) as a white powder. ¹H NMR (400 MHz, CDCl₃): δ 0.96 (app d, 6H, J_app = 6.4 Hz, CHMe₂), 1.04 (s, 9H, t-Bu), 1.34 (d, 3H, J = 7.3 Hz, Ala-β-Me), 2.08−2.16 (m, 3H, IPA-α,β-H), 2.17 (s, 3H, C(O)Me), 2.50 (dd, 1H, J = 7.0, 16.5 Hz, Asn(Me₂)-β-Hₐ), 2.94 and 3.00 (two s, 2 × 3H, NMe₂), 3.13 (dd, 1H, J = 3.2, 16.5 Hz, Asn(Me₂)-β-H_B), 4.23 (d, 1H, J = 8.6 Hz, TBG-α-H), 4.46 (app q⁵, 1H, J_app = 7.3 Hz, Ala-α-H), 4.85 (app dt, 1H, J_app = 3.2, 7.3 Hz, Asn(Me₂)-α-H), 6.10 (d, 1H, J = 8.6 Hz, TBG-NH), 7.47 (d, 1H, J = 8.0 Hz, Asn(Me₂)-NH), 7.65 (d, 1H, J = 7.0 Hz, Ala-NH). ¹³C NMR (100.6 MHz, CDCl₃): 16.73, 22.46, 22.51, 26.16, 26.28, 26.82, 34.43, 34.69, 35.53, 37.35, 46.16, 49.41, 54.97, 61.21, 170.44, 170.48, 171.06, 172.62, 206.55. MS: *m/z* (rel intensity) 427 (MH⁺, 100%), 340 ([MH⁺ − AlaMe], 10), 230 ([Asn-(Me₂)AlaMe + H⁺], 21), 198 (11),170 (18), 115 (67). IR: 1719 cm⁻¹. [α]²²D +49.5° (c 0.513, CHCl₃). UV: λ_max = 282 nm (ε = 48, MeOH). HRMS (C₂₁H₃₉O₅N₄) calcd 427.2920; found 427.2909. HPLC: system A >99%, system B >99%.

**Other Inhibitors, Substrates, and Intermediates.** The syntheses of activated carbonyl inhibitors **3**−**5** and **26**−**28** have been described.[13] Inhibitors **6** and **7** were prepared by the same published method as described for **4**; their physical constants are provided in the Supporting Information as are the full experimental procedures and characterization for intermediates **12**−**17**. The peptides **20** and **21** were prepared by standard solid-phase methods (respective purities of >96% and >97% by HPLC). The synthesis of β-lactam inhibitors **23**−**25** and the substrates **18**, **19**, and **22** have been described (see Table 5 for the respective references).

**Enzyme Assay and Kinetics.** All studies employed the HCMV protease mutant Ala143Gln to overcome the problem of autoproteolysis.[65] Full details of the preparation and purification of the recombinant enzyme (>99% purity) have been published.[12] IC₅₀ values were determined by using a fluorogenic assay that has also been described.[13] The kinetic parameters k_cat and K_M for the hydrolysis of **22** under varying salt conditions were determined by initial rate kinetics (according to ref 64) at 30 °C.

**Fluorescence Studies.** Fluorescence measurements were performed in 1 mL quartz cuvettes with a Perkin-Elmer LS-50B spectrofluorometer. Emission spectra of HCMV protease were recorded upon excitation at 280 nm. Further experimental details have been described.[12]

**NMR Studies: (a) Free Inhibitors in H₂O/DMSO.** Spectra of samples containing 30 mM MKs **1** and **2** and PFEKs **4**, **6**, and **7** in 15% H₂O in DMSO-d₆ were acquired on a Bruker DMX 600 instrument. Further experimental details are provided in the Supporting Information.

**(b) ROESY Experiments.** Homonuclear ROESY data from the States-TPPI method[66] were acquired at 600 MHz, cw spinlock, 300 t₁ data points from the addition of 32 transients, and a relaxation delay of 1.2 s. Three spectra were collected with spinlock times of 300 ms, 800 ms, and 1.5 s. ROESY data were also collected for 2 mM MKs **1** and **2** with a spinlock time of 300 ms.

**(c) Carbon-13 NMR.** One-dimensional ¹³C spectra for T₁ relaxation measurements for PFEKs **4**, **6**, and **7** were acquired at 150 MHz at 27 °C. Inversion recovery experiments were run with power-gated proton decoupling during acquisition. Ten spectra were acquired corresponding to the τ delays (0.01, 0.1, 0.25, 0.37, 0.5, 1.0, 1.5, 2.0, 3.0, and 7.0 s). Each spectrum was acquired by adding 1600 transients and using a relaxation delay of 6.9 s. The method used to calculate the T₁ values for the P1 and P4 α-centers of **6** and **7** is provided in the Supporting Information.

**(d) Transferred NOE Experiments.** Transferred NOESY experiments involving MK **2** were carried out on a Varian UNITY 750 instrument with mixing times of 50, 100, 150, and 250 ms. Sample preparation and NMR conditions were identical with those described in ref 17, as were the computational methods used to model MK **2** with Discover 95.0 and the CFF95 force field.

**Supporting Information Available:** Detailed procedures and characterization for compounds **12** to **17**, as well as characterization (NMR, MS, HPLC) of inhibitors **6** and **7**; details of NMR experiments; supporting NMR data (NOESY competition studies for MK **1** and quantitative comparison of cross-peak volumes for MK **2** (NOESY and ROESY) and **20** (NOESY)) (PDF). This material is available free of charge via the Internet at http://pubs.acs.org.

JA983904H

(65) Pinko, C.; Margosiak, S. A.; Vanderpool, D.; Gutowski, J. C.; Condon, B.; Kan, C.-C. *J. Biol. Chem.* **1995**, *270*, 23634−23640.
(66) Bax, A.; Davis, D. G. *J. Magn. Reson.* **1985**, *63*, 207−213.